© 2016. Published by The Company of Biologists Ltd | Development (2016) 143, 1971-1980 doi:10.1242/dev.132902

RESEARCH ARTICLE

Polycomb Ezh2 controls the fate of GABAergic neurons in the embryonic cerebellum

Xuesong Feng, Aster H. Juan, Hongjun A. Wang, Kyung Dae Ko, Hossein Zare and Vittorio Sartorelli*

ABSTRACT

Although the genetic interactions between signaling pathways and transcription factors have been largely decoded, much remains to be learned about the epigenetic regulation of cerebellar development. Here, we report that cerebellar deletion of Ezh2, the methyltransferase subunit of the PRC2 complex, results in reduced H3K27me3 and profound transcriptional dysregulation, including that of a set of transcription factors directly involved in cerebellar neuronal cell-type specification and differentiation. Such transcriptional changes lead to increased GABAergic interneurons and decreased Purkinje cells. Transcriptional changes also inhibit the proliferation of granule precursor cells derived from the rhombic lip. The loss of both cell types ultimately results in cerebellar hypoplasia. These findings indicate Ezh2/PRC2 plays crucial roles in regulating neurogenesis from both cerebellar germinal zones.

KEY WORDS: Polycomb, Ezh2, PRC2, Cerebellum, Neurogenesis, Purkinje cells

INTRODUCTION

During neural development, the proliferation and differentiation of progenitor cells is regulated to ensure that neuronal cell types are generated in a tightly controlled temporal sequence. This is guaranteed by combinatorial expression of transcription factors imparting cell type- and developmental-specific patterns. Increasing evidence indicates that histone post-translational modifications (PTMs) mediate the effects of transcription factors in dictating proper neural cell fate and neurodevelopment (Laugesen and Helin, 2014).

Tri-methylation of lysine 27 of histone H3 (H3K27me3) is associated with transcriptional repression in embryonic stem cells (Boyer et al., 2006; O'Carroll et al., 2001; Young, 2011) and tissues (Ezhkova et al., 2009; He et al., 2012; Juan et al., 2011; Snitow et al., 2015). This modification is mediated by the polycomb repressive complex 2 (PRC2) via its catalytic subunit enhancer of zeste 2 (Ezh2) (Cao et al., 2002; Kirmizis et al., 2004; Kuzmichev et al., 2002). The role(s) of Ezh2/PRC2 during neurodevelopment have been explored in a few contexts (Hirabayashi et al., 2009; Pereira et al., 2010) but further studies are needed for a detailed understanding of its function.

The embryonic cerebellum offers an ideal system in which to study neural fate commitment and differentiation because of its well-defined cytoarchitecture composed of few cell types. In the developing cerebellum, two distinct germinal zones give rise to all the neuronal subtypes. The ventricular zone generates GABAergic neurons, including inhibitory Purkinje cells and cerebellar interneurons (Golgi, basket and stellate cells). The anterior rhombic lip produces glutamatergic neurons such as granule cells, unipolar brush cells and excitatory deep cerebellar nuclei (Marzban et al., 2014; Roussel and Hatten, 2011; Zervas et al., 2005). Lineage tracing and birthdating studies have shown that cerebellar neurons are generated in a controlled spatial and temporal manner. A cadre of signaling molecules and transcription factors are involved in specifying the cerebellar primordium, neural lineage commitment, neuronal differentiation and cerebellar morphogenesis. Fibroblast growth factor 8 (Fgf8) and transcription factors Otx2, Gbx2, En1 and En2 are involved in the initial specification of the cerebellar primordium and cerebellar morphogenesis (Bilovocky et al., 2003; Cheng et al., 2010; Chi et al., 2003; Joyner et al., 1991; Li and Joyner, 2001; Meyers et al., 1998; Millen et al., 1994; Wurst et al., 1994), whereas transcription factors Ptf1a and Atoh1 are required for the commitment of neural lineages of the ventricular zone and rhombic lip, respectively (Wang et al., 2005; Hoshino et al., 2005; Machold and Fishell, 2005; Pascual et al., 2007). Transcription factor Pax2 is involved in both cerebellar primordium specification and interneuron commitment, albeit at different developmental stages (Bouchard et al., 2000; Maricich and Herrup, 1999; Weisheit et al., 2006). Transcription factor orphan nuclear receptor Rorα, and c-Ski family member and transcription regulator Corl2 (also known as Skor2), are both expressed in the Purkinje cells and are necessary for their differentiation and maturation (Gold et al., 2003; Hamilton et al., 1996; Minaki et al., 2008; Nakagawa et al., 1997; Nakatani et al., 2014). Mutations of these signaling molecules and transcription factors often lead to congenital cerebellar conditions including cerebellar agenesis and hypoplasia that is associated with Dandy–Walker syndrome (Gold et al., 2003; Hamilton et al., 1996; Millen et al., 2014; Nakagawa et al., 1997; Parisi and Dobyns, 2003). Therefore, it is pivotal to understand how these signaling molecules and transcription factors are regulated during cerebellar development.

In this study, we explored the function of Ezh2/PRC2 in the murine embryonic cerebellum by genetically inactivating Ezh2 in the cerebellar primordium and found that the mutant mice exhibited cerebellar hypoplasia. Using a combination of genome-wide approaches, we unveiled a network of gene expression and chromatin modifications underlying the phenotypic changes occurring in the absence of Ezh2. These findings indicate that Ezh2/PRC2 serves as a 'gatekeeper' to govern proper cerebellar neurogenesis in both cerebellar germinal zones.

RESULTS

Deletion of Ezh2 in the cerebellar primordium

To address the role of PRC2 in the developing cerebellum, we selectively excised the *Ezh2* gene by crossing *Ezh2*$^{fl/fl}$ mice (Su et al.,

Laboratory of Muscle Stem Cells and Gene Regulation, National Institute of Arthritis, Musculoskeletal and Skin Diseases (NIAMS), National Institutes of Health, 50 South Drive, Bethesda, MD 20892, USA.

*Author for correspondence (sartorev@mail.nih.gov)

V.S., 0000-0002-9284-3675

Received 10 November 2015; Accepted 6 April 2016

Development (2016) 143, 1971-1980 doi:10.1242/dev.132902

2003) with *Pax7-Cre* mice (Keller et al., 2004) to generate the conditional null genotype *Pax7-Cre; Ezh2$^{fl/fl}$*. For convenience, we named these conditional knockout (cKO) mice Ezh2^{cKO}. The Ezh2^{cKO} mice display skeletal muscle defects resulting from Pax7 expression and Ezh2 deletion in adult muscle stem cells (satellite cells) (Juan et al., 2011; Woodhouse et al., 2013). In addition to satellite cells (Jostes et al., 1990; Seale et al., 2000), Pax7 expression is also observed in the dorsal neural tube (Jostes et al., 1990). Cells with floxed alleles created by *Pax7-Cre* expression are inherited in dorsal neural tissues including the whole cerebellar primordium (Keller et al., 2004). We started investigating Ezh2 and Pax7 expression by immunostaining the cerebella of embryonic day (E) 10.5 embryos (Fig. 1). At this stage, Ezh2 was detected in almost every nucleus of the whole embryonic brain. Consistent with previous reports (Keller et al., 2004), Pax7 expression was restricted to the dorsal region (Fig. 1). At both E10.5 (Fig. 1) and E11.5 (data not show), Ezh2 expression was comparable between Ezh2^{cKO} and littermate controls in the cerebellum. Transient retention of Ezh2 protein in the nuclei of cells expressing Cre-recombinase was reported when *Ezh2* was genetically deleted in the cerebral cortex

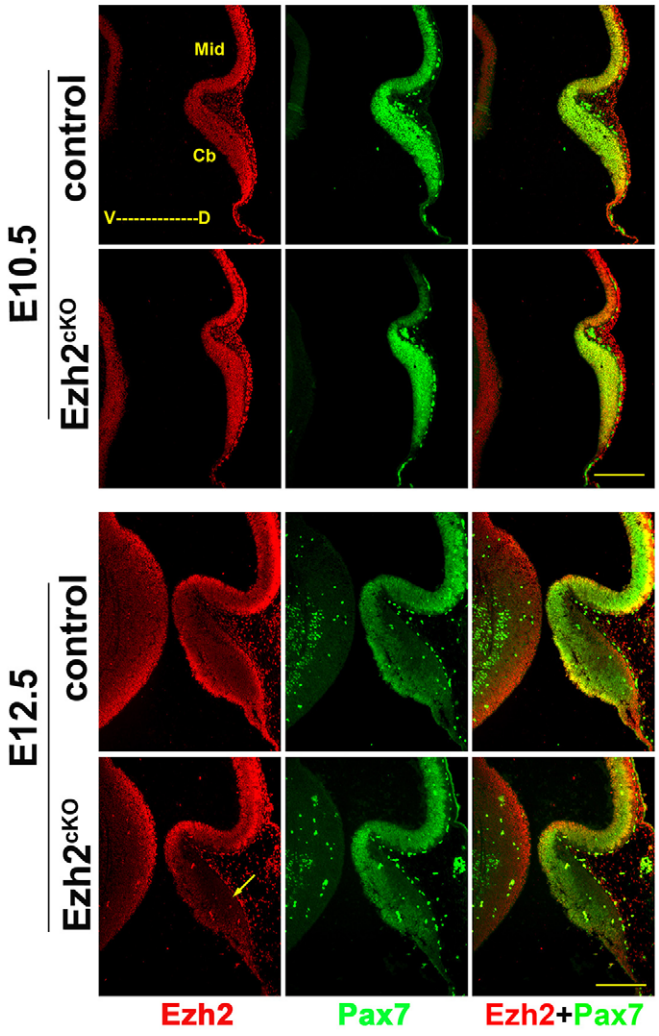

Fig. 1. Ezh2 and Pax7 are abundantly expressed in the cerebellar primordium. Ezh2 and Pax7 immunofluorescence staining in both Ezh2^{cKO} and littermate control cerebella at early embryonic stages E10.5 (top panels) and E12.5 (bottom panels). Mid, midbrain; Cb, cerebellum. for all panels, ventral (V) to the left, dorsal (D) to the right. Arrow indicates Cb region. Scale bar: 200 µm.

(Pereira et al., 2010). Reduced Ezh2 expression in the cerebellar primordium of Ezh2^{cKO} mice was noted starting from E12.5 (Fig. 1). In agreement with decreased Ezh2 accumulation, H3K27me3 was reduced at E12.5 and by E14.5 very few cells remained H3K27me3-positive in the Ezh2^{cKO} cerebellum (Fig. 2A,B). Consistent with the selective expression of Pax7 in the dorsal structures (Fig. 1), H3K27me3 was not apparently affected in the ventral part of the Ezh2^{cKO} embryonic brain (Fig. 2B, arrows).

Ezh2^{cKO} mice exhibit developmental cerebellar defects and hypoplasia

Because reduction of Ezh2 and H3K27me3 in the cerebellar primordia began at around E12.5, we investigated possible developmental defects by histology analysis comparing the morphology between Ezh2^{cKO} mice and littermate controls from E12.5 onward. At E15.5, the cerebellar anlage of Ezh2^{cKO} embryos was discernibly smaller, missing the characteristic budding external granular layer (EGL) emerging from the rhombic lip (Fig. 2C). This phenotype became more evident during development and by E17.5, Ezh2^{cKO} embryos had a much smaller cerebellum lacking a distinct EGL (Fig. 2C). Gross cerebellar defects were evident in postnatal day (P)8 pups with the cerebellum of Ezh2^{cKO} mice lacking majority of the vermis (Fig. 2D, upper panel). A para-sagittal section through the hemisphere region of the cerebellum showed that the foliation pattern in Ezh2^{cKO} mice was much less intricate than that of littermate controls (Fig. 2D, lower panel). These defects persisted throughout adulthood. Nissl staining documented impoverished foliation (Fig. S1A) and magnetic resonance imaging (MRI) confirmed absence of the cerebellar vermis in adult Ezh2^{cKO} mice (Fig. S1B).

Ezh2 controls expression of cerebellar developmental regulators

The phenotypic defects of the Ezh2^{cKO} embryos prompted us to investigate the functional consequences of Ezh2 deletion on the cerebellar transcriptome and epigenome. Therefore, RNA-seq and H3K27me3 ChIP-seq were conducted on E13.5 cerebella from Ezh2^{cKO} mice and littermate controls. To precisely identify and isolate Pax7-Cre-expressing regions, we generated a reporter mouse by breeding the *Rosa26-YFP* locus (Srinivas et al., 2001) into Ezh2^{cKO} mice to obtain Ezh2$^{cKO:YFP}$ mice. YFP-positive cerebella were identified and isolated under a fluorescence dissecting microscope (Fig. S2A,B).

Analysis of the H3K27me3 ChIP-seq datasets revealed that the H3K27me3 mark was enriched at ∼13,000 genomic regions. More specifically, H3K27me3 peaks were present at ∼5700 intergenic, ∼2200 intragenic (including gene body and introns), as well as ∼4000 promoter regions (±2000 bp from the transcription start site, TSS) (Fig. 3A). In Ezh2^{cKO} cerebellar genomes, H3K27me3 was largely reduced compared with those of control embryos (Fig. 3A; Table S1). Gene ontology analysis of the genes associated with H3K27me3^{+} TSS returned terms related to ‘developmental protein’, ‘homeobox’, ‘DNA binding’ and ‘transcription regulation’ (Fig. 3B). Among H3K27me3^{+} TSS, there were those corresponding to genes for transcription factors involved in either conferring cell pluripotency (*Nanog*) or regulating differentiation of non-neuronal cell lineages, such as *Myod1* (skeletal muscle), *Hand1* and *Hand2* (neural crest and the second heart field), *Nkx2* and T-box genes (mesoderm), and over 150 homeobox-containing genes including *HoxA*, *-B*, *-C* and *-D* clusters (Table S1). In addition, promoters of genes encoding transcription factors and signaling regulators crucial for cerebellar development were H3K27me3^{+}.

Development (2016) 143, 1971-1980 doi:10.1242/dev.132902

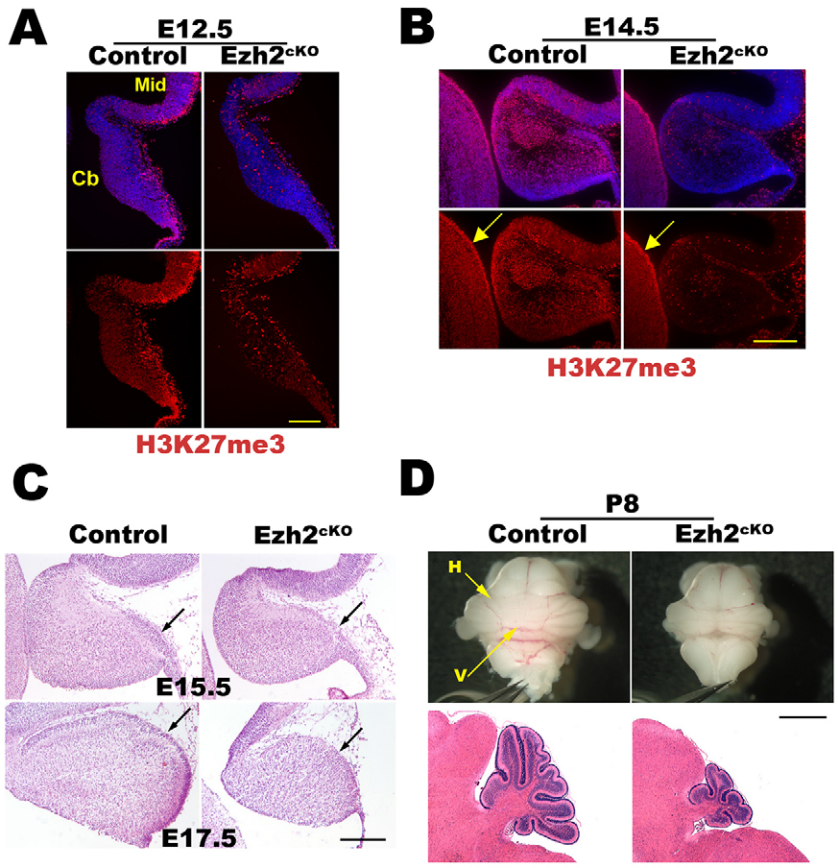

Fig. 2. Cerebellar gene ablation of Ezh2 induces decreased H3K27me3 and developmental defects. (A,B) Embryonic brain sagittal sections of Ezh2^{cKO} and littermate control embryos at E12.5 (A) and E14.5 (B) were immunostained with an anti-H3K27me3 antibody and counterstained with DAPI to highlight the nuclei. Arrows in B indicate brain ventral regions. (C) H&E histology staining of E15.5 (top) and E17.5 (bottom) cerebellar para-sagittal sections from control and Ezh2^{cKO} cerebella. Arrows indicate the EGL. (D) Dorsal views of P8 control and Ezh2^{cKO} cerebella (top panel). H&E histology staining of para-sagittal sections through the hemisphere of P8 control and Ezh2^{cKO} cerebella (lower panel). Mid, midbrain; Cb, cerebellum; V, vermis; H, hemisphere. For all panels, ventral to the left, dorsal to the right. Scale bars: 200 µm in A-C; 800 µm in D, lower panel.

These included *Ptf1a*, *Atoh1*, *En1*, *Otx2*, *Gbx1/2*, *Gli1/3*, *Lhx1/2/5*, *Pax2/5/8*, *Hoxa1/2*, *Zic1/2* and 32 members of the *Wnt* and *Fgf* families (Fig. 3C; Table S1). Overall, these findings suggest a potential role of H3K27me3 in regulating a large number of non-neuronal as well as neuronal developmental transcription factors.

Analysis of RNA-seq datasets revealed that 481 transcripts were upregulated and 98 transcripts were downregulated in E13.5 cerebella of Ezh2^{cKO} embryos compared with littermate controls (Fig. 4A; Table S2). Of the 481 upregulated genes, ∼70% (339/481) were occupied by H3K27me3 (Fig. 4B; Table S3), indicating that these genes might be directly repressed by H3K27me3 in normal development. Most of the genes whose promoters were marked by H3K27me3 and that were related to non-neuronal cell lineage specification remained repressed in spite of decreased H3K27me3 in Ezh2^{cKO} embryos (*Myod1*, *Mef2d*, *Gata2-6*, *Hand1*). This indicates that at this developmental stage, cerebellar cells have already committed to the neural fate, and that reducing H3K27me3 is not sufficient to derepress non-neural lineage regulators. Gene ontology analysis of the 481 upregulated transcripts in Ezh2^{cKO} cerebella returned terms such as 'developmental protein', 'homeobox', 'transcription regulation' and 'DNA binding' (Fig. 4C; Table S4). Inspection of the gene ontology terms enriched in Ezh2^{cKO} embryos permitted the identification of 87 transcripts encoding transcription factors (Fig. S3). This class of transcripts corresponds to 18% (87/481) of the total genes upregulated in Ezh2^{cKO} embryos, suggesting a relevant role of Ezh2 in top-down control of developmental regulators.

Among these transcripts, transcription factors involved in ventricular zone neurogenesis, particularly in Purkinje cell and cerebellar interneuron specification and commitment, showed significant expression changes in the Ezh2^{cKO} cerebella (Fig. S3). Cerebellar interneuron marker genes (*Pax2*, *Pax5*, *Pax8*) were upregulated by ∼twofold, whereas genes known to be involved in Purkinje cell commitment (*Rora*, *Olig2*, *Olig1*) were downregulated by ∼twofold (Fig. S3; Table 1), suggesting an irregular fate transition between these two neuronal subtypes in Ezh2^{cKO} cerebella.

Loss of Ezh2 leads to decreased number of Purkinje cells and gain of cerebellar interneurons

Out of 98 downregulated transcripts in Ezh2^{cKO} cerebella, 50 (54%) were identified as components of the gene ontology term 'membrane' (*P*-value: 9.7×10^{-8}) (Table S5). Analysis of these transcripts revealed that they are involved in regulating Purkinje cell adhesion, migration and dendrite projection (Table S6). Furthermore, other known Purkinje cell markers (*Skor2*, *Foxp2*, *Pcp4*) were also downregulated (Table 1). These findings suggested a potential loss of Purkinje cells in Ezh2^{cKO} cerebella. To evaluate this possible phenotype, we investigated the number and distribution of cerebellar interneurons and Purkinje cells in both Ezh2^{cKO} cerebella and in littermate controls. E13.5 and E14.5 cerebella sagittal sections were immunostained with antibodies against Pax2 and Rorα to identify interneurons and Purkinje cells, respectively (Fig. 5A-D). Pax2^{+} cells were increased in Ezh2^{cKO} cerebella, adopting a deeper position similar to that normally observed at later stages of development (Englund et al., 2006) (Fig. 5A,C). By contrast, while being correctly positioned in the deep part of cerebellar primordium of both genotypes, Rorα^{+} Purkinje cells were decreased in the Ezh2^{cKO} cerebella (Fig. 5B,D). In addition, to quantify the Pax2^{+} and Rorα^{+} cells of the whole cerebellar primordium, we FACS-sorted YFP^{+} cells from Ezh2$^{cKO:YFP}$ cerebella and littermate controls at E13.5 (Fig. S2B,C). YFP^{+} cells were plated and fixed immediately, then immunostained

Development (2016) 143, 1971-1980 doi:10.1242/dev.132902

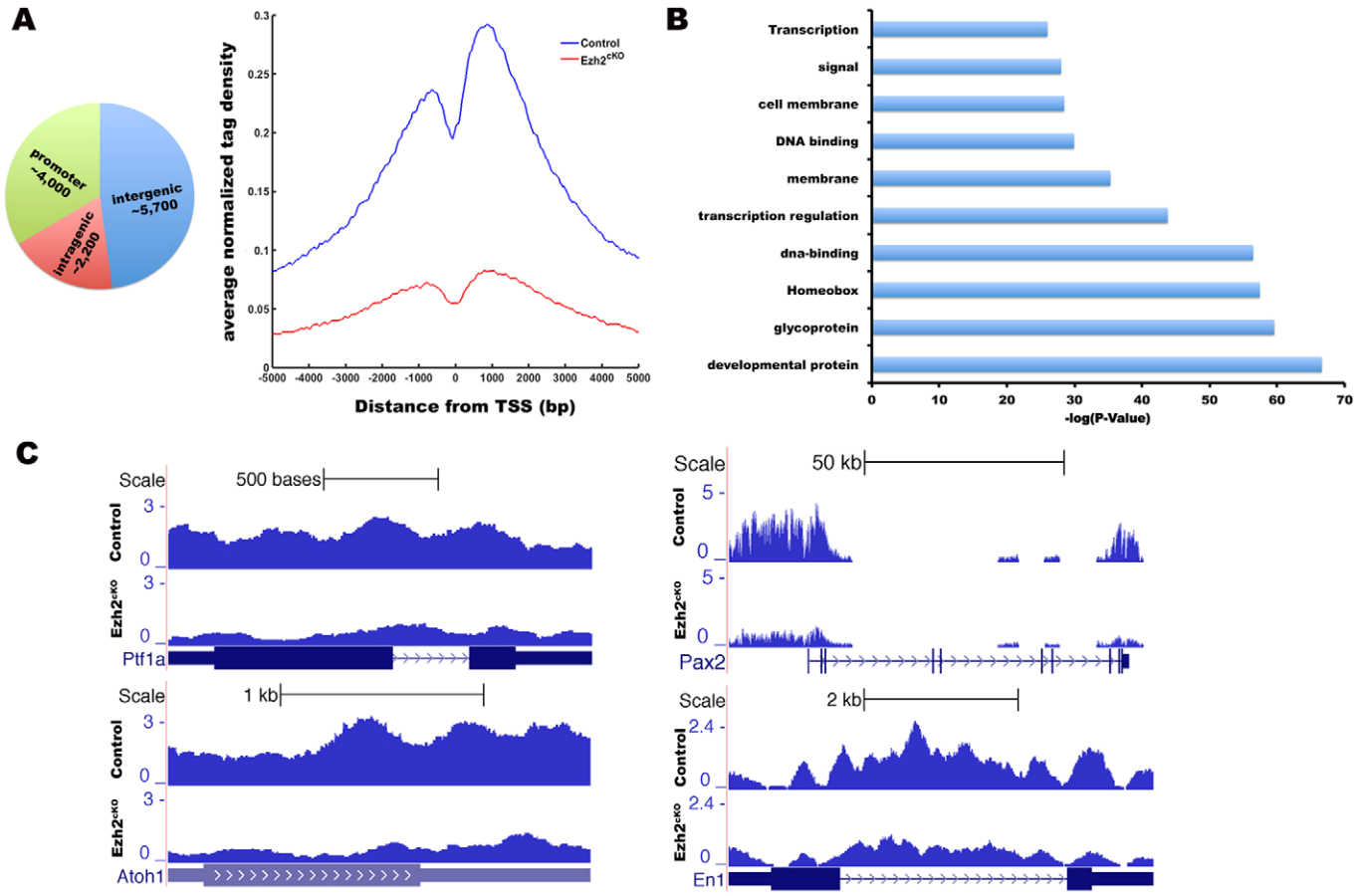

Fig. 3. H3K27me3 genome-wide distribution. (A) Genomic H3K27me3 peak distribution in E13.5 control cerebellum (left panel) and average (global) H3K27me3 tag density in control (blue line) and Ezh2^{cKO} (red line) cerebella (right panel). H3K27me3 ChIP-seq was repeated with cerebella of two control and two Ezh2^{cKO} embryos (*n*=2). (B) Gene ontology analysis of genes corresponding to H3K27me3 promoter regions. (C) Genome browser views of H3K27me3 ChIP-seq traces on representative genes *Pft1a*, *Atoh1* (left panels) *Pax2* and *En1* (right panels) involved in cerebellar neurogenesis in control and Ezh2^{cKO} cerebella.

with antibodies against Pax2 and Rorα (Fig. S4A,B). After normalizing for total DAPI^{+} nuclei, cells from Ezh2$^{cKO:YFP}$ cerebella were found to contain a higher percentage of Pax2^{+} cells and lower percentage of Rorα^{+} cells (Fig. S4A,B, graphs). Taken together, these findings showed that loss of Ezh2 lead to the loss of Purkinje cells and gain of cerebellar interneurons at early embryonic stages.

Transcriptional derepression of the *Ink4B-Arf-Ink4A* locus and cerebellar proliferation defects in Ezh2^{cKO} mice

Ezh2 regulates cell proliferation through repression of the *Ink4B-Arf-Ink4A* tumor suppressor locus (also known as the *Cdkn2b-Cdkn2a* locus) in cultured cells and tissues (Bracken et al., 2007; Ezhkova et al., 2009; Juan et al., 2011). Because of the EGL reduction and cerebellar hypoplasia (Fig. 2C,D), we queried expression and H3K27me3 occupancy of the *Ink4B-Arf-Ink4A* locus. Expression of the individual components of the *Ink4B-Arf-Ink4A* locus, *Cdkn2a*, *Cdkn2b* and *Cdkn2c*, was increased and their H3K27me3 occupancy was reduced in Ezh2^{cKO} cerebella (Fig. 6A). As determined by quantitative PCR (qPCR), *Cdkn2a* expression remained elevated in E13.5-E15.5 Ezh2^{cKO} cerebella (Fig. 6B). Cdkn2a levels were increased in regions corresponding to the EGL and deep cerebellar nuclei of E17.5 Ezh2^{cKO} mice (Fig. S5). Consistent with transcriptional derepression, H3K27me3 was decreased at the *Cdkn2a* promoter regions of Ezh2^{cKO} cerebella at E13.5 and E14.5 (Fig. 6B). We confirmed the EGL phenotype (Fig. 2C,D) by immunostaining for the granule precursor cell (GPC) marker Pax6 (Fig. 6C) (Engelkamp et al., 1999). At E14.5, Ezh2^{cKO} cerebella had comparable number of Pax6^{+} GPCs as control cerebella. However, at E15.5, the EGL in Ezh2^{cKO} was dramatic reduced in thickness. The number of Pax6^{+} GPCs was largely reduced in Ezh2^{cKO} cerebella (Fig. 6C), indicative of either cell death or lack of cell proliferation. As *Cdkn2a* acts as a potent cell-cycle inhibitor of the G1-S transition (Nobori et al., 1994), we evaluated the proliferative state of EGL by EdU labeling (Zeng et al., 2010). We administrated EdU in pregnant mice at E13.5 (Fig. 7A) and E14.5 (Fig. 7B), respectively, and collected embryos after 24 h. Co-staining the embryonic brain sections with EdU and anti-Ki67 (mitotic marker) antibody revealed the proliferation state of EGL. We found that ~55% EdU^{+} cells had already exited the cell cycle in E14.5 Ezh2^{cKO} EGL, whereas ~85% EdU^{+} cells still maintained proliferative state in controls (Fig. 7A). At E15.5, ~80% EdU^{+} cells exited the cell cycle in Ezh2^{cKO} EGL, while ~94% EdU+ cells still maintained proliferative state in controls (Fig. 7B). Apoptosis, evaluated by TUNEL assay, was not increased in Ezh2^{cKO} cells (Fig. S6). Thus, reduced proliferation, rather than cell death, appears to be responsible for decreased representation of granule precursor cells in Ezh2^{cKO} cerebella.

DISCUSSION

In this study, we found that Ezh2 regulates embryonic cerebellum development by affecting the emergence of distinct neuronal cell types. Ezh2 ablation resulted in increased Pax2^{+} interneurons,

Development (2016) 143, 1971-1980 doi:10.1242/dev.132902

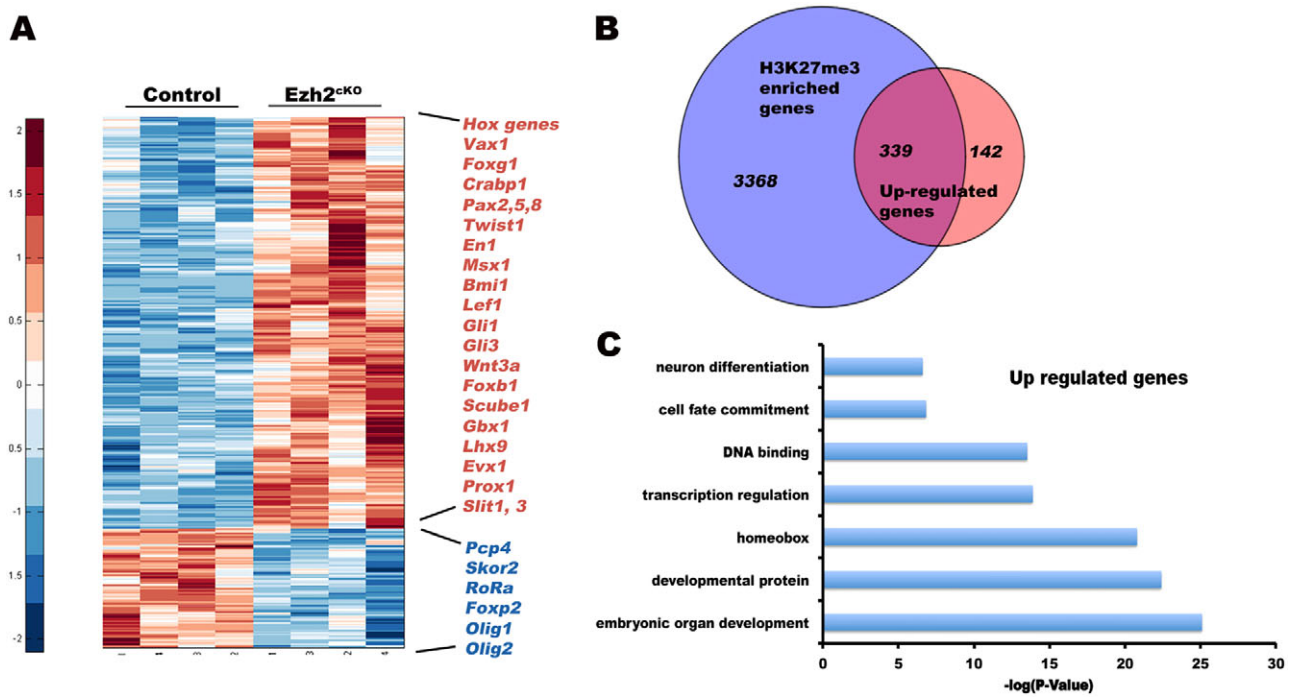

Fig. 4. Transcriptional dysregulation in Ezh2^{cKO} embryos. (A) Gene expression changes in E13.5 control and Ezh2^{cKO} cerebella. A list of selected up- and downregulated transcripts is indicated. RNA-seq was repeated with cerebella of four control and four Ezh2^{cKO} cerebella (*n*=4). (B) Venn diagram of H3K27me3 promoter regions in control and upregulated genes in Ezh2^{cKO} cerebella. (C) Gene ontology terms of 481 upregulated genes in E13.5 Ezh2^{cKO} cerebella.

reduced representation of Rorα^{+} Purkinje cells and granule precursor cells, and ultimately in a hypoplastic cerebellum. Bmi1, a member of the polycomb repressive complex 1 (PRC1) has been reported to play an important role in the expansion of granule precursor cells (Leung et al., 2004). However, PRC1 does not seem to control Purkinje cell formation and differentiation (Leung et al., 2004), suggesting that PRC1 and PRC2 exert distinct functions during cerebellar neurogenesis.

Table 1. Expression change and H3K27me3 occupancy of genes known to be involved in early embryonic cerebellar development

Gene name	Fold-change	*P*-value	H3K27me3	References
Early cerebellar specification and patterning				
Fgf8*	5.05 ↔	0.111	+	(Crossley et al., 1996; Liu and Joyner, 2001; Martinez et al., 1999)
Otx2*	2.50 ↔	0.095	+	(Li and Joyner, 2001)
Gbx2	1.07 ↔	0.504	+	(Li and Joyner, 2001; Liu and Joyner, 2001)
En1	1.38 ↑	0.021	+	(Joyner et al., 1991)
En2	1.01 ↔	0.875	–	(Joyner et al., 1991; Millen et al., 1995)
Ventricular zone-derived cell lineage specification and commitment				
Neurog1	0.96 ↔	0.896	+	(Dalgard et al., 2011; Kim et al., 2011)
Ascl1	1.11 ↔	0.611	–	(Sudarov et al., 2011)
Lhx1	0.79 ↓	0.041	+	(Pillai et al., 2007; Zhao et al., 2007)
Lhx5	0.88 ↔	0.245	+	(Pillai et al., 2007; Zhao et al., 2007)
Ptf1a	0.68 ↓	0.029	+	(Millen et al., 2014; Sellick et al., 2004)
Olig1	0.47 ↓	0.033	+	(Seto et al., 2014)
Olig2	0.53 ↓	3.1E-06	+	(Seto et al., 2014)
Gsx1	1.22 ↔	0.324	+	(Seto et al., 2014)
Interneuron lineage and differentiation				
Pax2	1.92 ↑	0.001	+	(Maricich and Herrup, 1999; Pillai et al., 2007; Seto et al., 2014)
Pax5	1.94 ↑	0.011	+	(Pillai et al., 2007)
Pax8	5.78 ↑	5.8E-06	+	(Pillai et al., 2007)
Purkinje cell lineage and differentiation				
Pcp4	0.54 ↓	0.004	–	(Wei et al., 2011)
Rorα	0.52 ↓	0.003	–	(Gold et al., 2003; Hamilton et al., 1996)
Skor2	0.52 ↓	0.005	+	(Nakatani et al., 2014)
Foxp2	0.72 ↓	0.012	+	(Fujita and Sugihara, 2012)

Fold-change: mean of RPKMs of Ezh2cKO/Control.
↑, upregulated; ↓, downregulated; ↔, no change (*P*<0.05; *t*-test).
* These genes showed fold-changes greater than 1.5 times up- or downregulated, but were not statistically significant (*P*>0.05; *t*-test), mostly resulting from the very low expression level in both genotypes.
+, promoter was occupied by H3K27me3 in control.
–, promoter was not occupied by H3K27me3 in control.

Development (2016) 143, 1971-1980 doi:10.1242/dev.132902

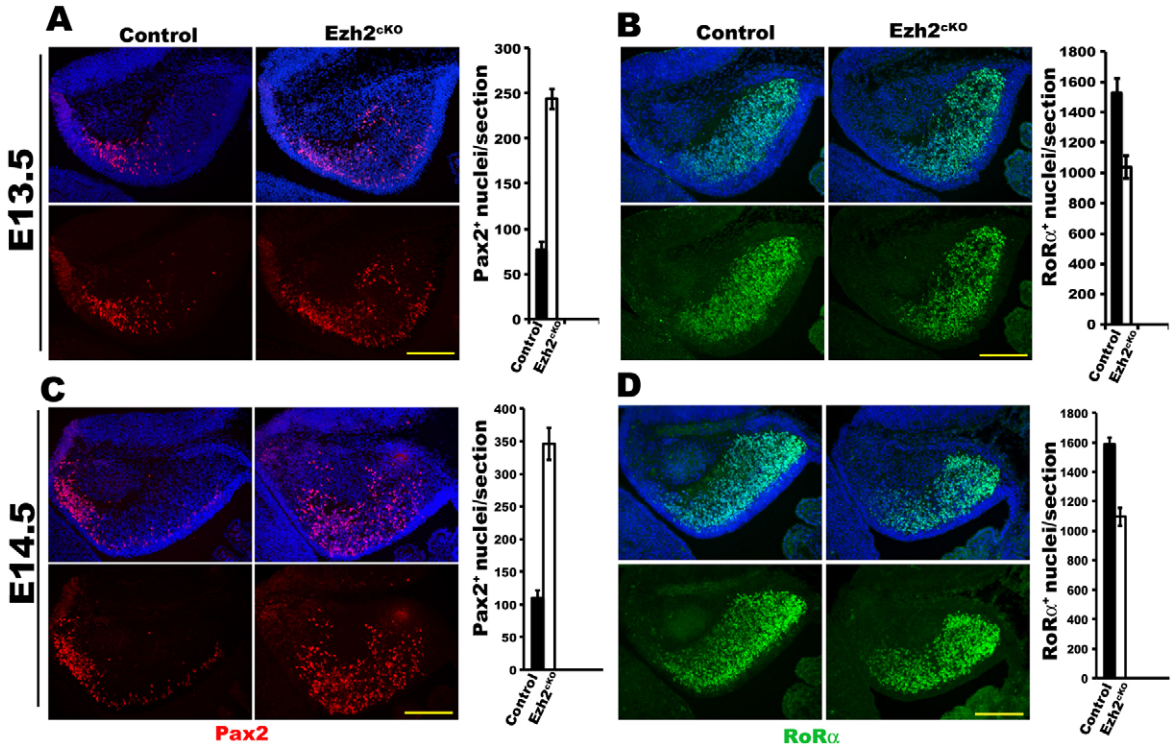

Fig. 5. Pax2^{+} interneurons are increased whereas Rorα^{+} Purkinje cells are decreased in Ezh2^{cKO} cerebella. (A) E13.5 para-sagittal sections were immunostained with anti-Pax2 (red) antibody and counter-stained with DAPI (blue) showing ectopic Pax2 expression in control and Ezh2^{cKO} cerebella. (B) E13.5 para-sagittal sections were immunostained with anti-Rorα antibody (green) and counter-stained with DAPI (blue), showing the Rorα^{+} cells were distributed in a more compact manner in control than in Ezh2^{cKO} cerebella. (C,D) Similar phenotypes were observed in E14.5 para-sagittal sections stained for Pax2 (C) and Rorα (D). The number of Pax2- and Rorα-positive nuclei on each section was quanitified and graphed on the right side of each image (n=3), P-value was calculated by paired t-test: A, P≈0.003; B, P≈0.006; C, P≈0.003; D, P≈0.002. Error bars represent mean±s.e.m. Anterior to the left, posterior to the right in all images. Scale bars: 200 µm.

We employed a genome-wide approach to survey gene expression changes resulting from the knockout of *Ezh2*. Analysis of genes involved in early embryonic cerebellum development (E8.5 to ~E13.5) revealed developmental dependency on Ezh2/PRC2 (Table 1). Even though occupied by H3K27me3, expression of genes controlling cerebellar specification and patterning developmental events occurring at earlier stages (E8.5-9.5), was not affected in Ezh2^{cKO} embryos (Table 1). This is likely a result of the fact that H3K27me3 accumulation was affected starting from E12.5 in Ezh2^{cKO} cerebella (Fig. 1A), at which stage the primordium has already been committed to cerebellar fate (Zervas et al., 2005). By contrast, genes involved in interneuron and Purkinje cell commitment and differentiation were upregulated and downregulated, respectively (Table 1, Fig. 5). These events occurred at E13.5, a critical developmental stage when ventricular zone precursor cells undergo a Purkinje cell-to-interneuron fate transition (Martinez et al., 2013). Taken together, these observations indicate that Ezh2/PRC2 regulates cerebellum development in a cell stage-dependent manner.

Purkinje cells and cerebellar interneurons derive from Ptf1a^{+} neural precursors in a temporally controlled manner through mechanisms that remain to be fully understood. Among Ptf1a^{+} ventricular zone precursors, Olig1/2^{+} and Gsx1^{+} precursor cells are commited to develop into Rorα^{+} Purkinje cells and Pax2^{+} interneurons, respectively. Olig1/2 and Gsx1 mutually represses each other during this temporal transition (Seto et al., 2014). Our study suggests a potential mechanism regulated by Ezh2 in controlling generation of Purkinje cells and cerebellar interneurons. Reduced H3K27me3 following *Ezh2* knockout resulted in increased expression of Pax2 and generation of Pax2^{+} interneurons in Ezh2^{cKO} cerebella. Increased Pax2 expression might accelerate the turnover process from Gsx1^{+} precursor cells to Pax2^{+} interneurons, which in turn would counteract the generation of Olig1/2^{+} precursors and Rorα^{+} Purkinje cells.

An additional phenotype observed in Ezh2^{cKO} cerebella was the decreased proliferation of granule precursor cells of the EGL. Granule precursor cells contribute to the proper cerebellar growth and shape up the foliation pattern throughout embryonic and early postnatal stages (Martinez et al., 2013; Zervas et al., 2005). Purkinje cells are essential for granule cell proliferation through secretion of the mitogen Shh (Corrales et al., 2004; Lewis et al., 2004) and loss of Purkinje cells leads to cerebellar hypoplasia, as seen in Rorα and Skor2 mutant mice (Gold et al., 2003; Hamilton et al., 1996; Nakagawa et al., 1997; Nakatani et al., 2014). A similar phenotype occurred in Ezh2^{cKO} mice (Fig. 2D; Fig. S1). Combined with proliferation defects of granule cells associated with overexpression of *cdkn2a*, *-b* and *-c* at early embryonic stages (Fig. 6), loss of Purkinje cells in Ezh2^{cKO} mice would ultimately lead to a hypoplastic cerebellum. Elevated Ezh2 has been reported to be involved in the pathogenesis of ataxia-telengiectasia (A-T) caused by ATM protein deficiency. A-T postmitotic neurons have increased PRC2 and undergo cell death, indicating that controlled Ezh2 expression is crucial for neuronal function and survival (Li et al., 2013). Thus, in addition to its role in orchestrating topographic migration and connectivity of precerebellar neurons (Di Meglio et al., 2013) and neuron survival (Li et al., 2013), this study indicates that Ezh2 regulates gene expression patterns underlying the appropriate temporal neurogenesis required for proliferation and differentiation of neural precursor cells.

Development (2016) 143, 1971-1980 doi:10.1242/dev.132902

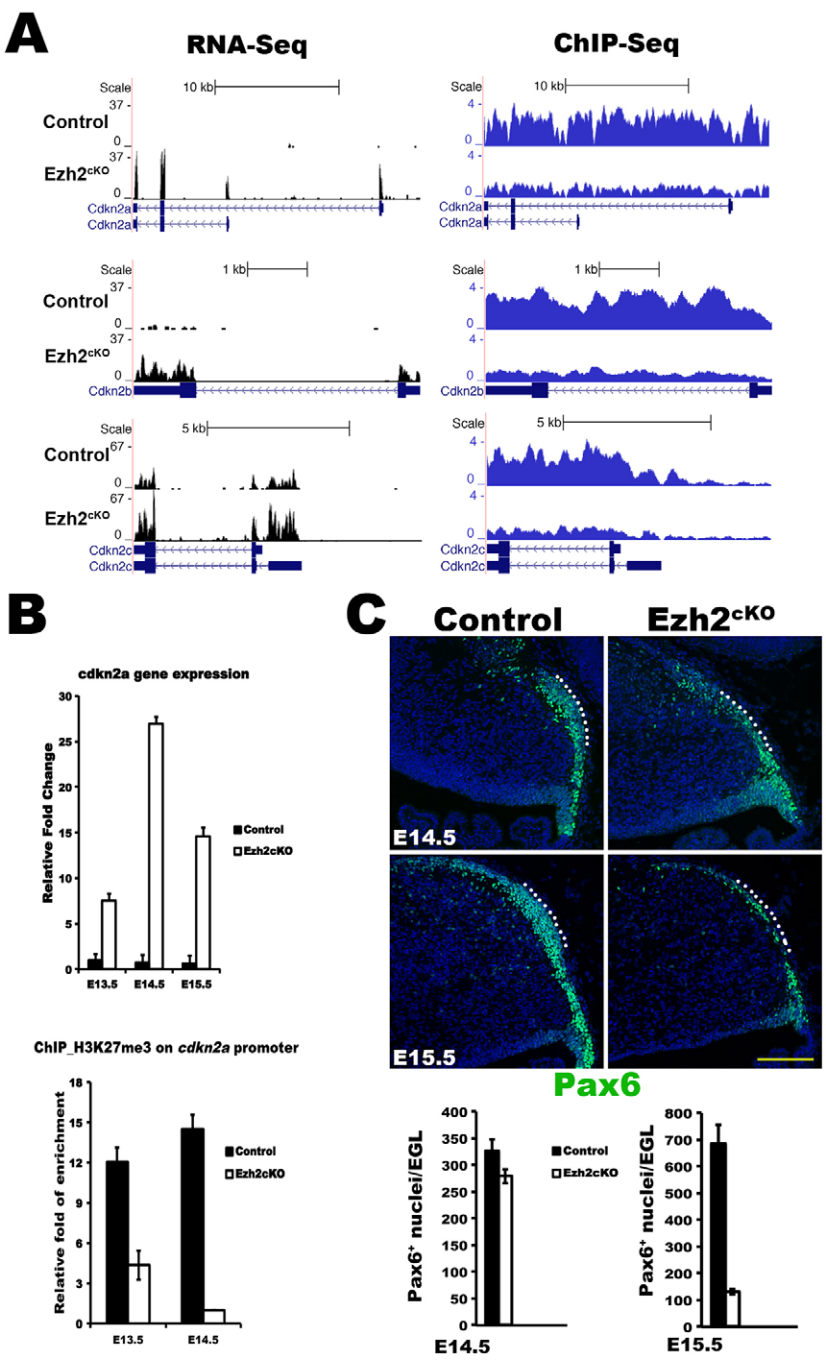

Fig. 6. Derepression of the *Ink4B-Arf-Ink4A* tumor suppressor locus and cell proliferation defects in Ezh2^{cKO} embryos. (A) RNA-seq (left panels) and H3K27me3 ChIP-seq (right panels) UCSC genome browser tracks for *cdkn2a*, *-b* and *-c* in Ezh2^{cKO} and littermate control embryos. (B) Relative expression (qPCR, top panel) and H3K27me3 promoter enrichment (ChIP-qPCR, bottom panel) for the *Cdkn2a* gene through embryonic stages in Ezh2^{cKO} and littermate control embryos. Experiments were performed with three biological replicates (n=3). Error bars represent mean±s.e.m. (C) Cerebellar sagittal sections at E14.5 (top panels) and E15.5 (bottom panels) of Ezh2^{cKO} and littermate control embryos were immunostained with anti-Pax6 antibody (green) counterstained with DAPI (blue). Pax6^{+} cells were quantified and graphed below the images (n=3), P-value was calculated by paired t-test: E14.5, $P\approx0.09$; E15.5, $P\approx0.003$. Dotted lines indicate the pial surface, the areas correspond to the areas in Fig. 7. Scale bar: 100 µm.

MATERIALS AND METHODS

Mice and animal care

Mice were housed in a pathogen-free facility and all experiments were performed according to the National Institutes of Health (NIH) Animal Care and Use regulations. *Pax7$^{+/Cre}$:Ezh2$^{fl/fl}$* mice (Ezh2 conditional knockout, Ezh2^{cKO}) were generated by breeding *Pax7-Cre* mice (*Pax7$^{+/Cre}$*) (Keller et al., 2004) with Ezh2 flox allele mice (*Ezh2$^{fl/fl}$*) (Su et al., 2003). We crossed *Rosa26-YFP* (*Rosa26-YFP$^{Y/Y}$*) mice (Srinivas et al., 2001) to *Ezh2$^{fl/fl}$* for three generations to homozygosity (*Ezh2$^{fl/fl}$:Rosa26-YFP$^{Y/Y}$*) . *Ezh2$^{fl/fl}$:Rosa26-YFP$^{Y/Y}$* females were mated with heterozygous males (*Pax7$^{+/Cre}$:Ezh2$^{fl/+}$*) to obtain *Pax7$^{+/Cre}$:Ezh2$^{fl/fl}$:Rosa26$^{YFP/+}$* (Ezh2$^{cKO:YFP}$) mice. Timed matings were carried out with heterozygous *Pax7$^{+/Cre}$:Ezh2$^{fl/+}$* males crossed with homozygous females (either *Ezh2$^{fl/fl}$* or *Ezh2$^{fl/fl}$:Rosa26$^{YFP/YFP}$*). The day a vaginal plug was observed in females was counted as embryonic day 0.5. Genotypes were identified by allelic PCR on embryonic tissues or tail genomic DNA. Genotyping protocol and primers were described by Juan et al. (2011).

Embryo dissection and imaging

E10.5 to E17.5 embryonic brains were dissected under either white-field or fluorescence dissecting microscopes (Olympus SZX9, Leica Fluro). The genotypes were identified by allelic PCR on genomic DNA of embryonic tissues (tails and limbs). The embryonic brains were further fixed in 4% PFA and processed for paraffin- (E10.5-12.5) and/or cryo- (E12.5-17.5) embedding for histology and immunohistochemistry. The P8 brains were dissected out from pups and fixed in 4% PFA and processed for paraffin embedding. The E13.5 cerebellar primordia for RNA-seq and ChIP-seq experiments were precisely dissected under a fluorescence microscope based on the area with YFP expression. The meninges were removed and discarded. Images of histology and

Development (2016) 143, 1971-1980 doi:10.1242/dev.132902

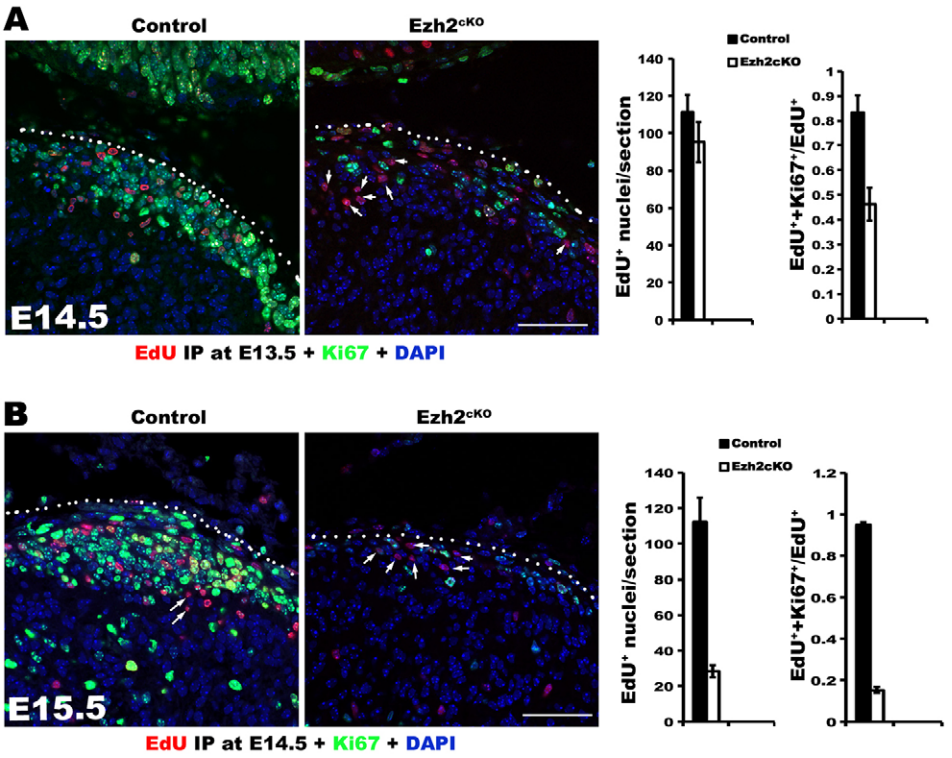

Fig. 7. Reduced proliferation of granule precursor cells in the EGL of Ezh2^{cKO} embryos. (A,B) EdU was administrated by intraperitoneal injection on pregnant mice at E13.5 (A) and at E14.5 (B). The embryos were collected 24 h after the treatment. EdU (red) and Ki67 (green) immunofluorescence staining was analyzed on para-saggital sections. Each section was counterstained with DAPI (blue). EdU-positive nuclei (EdU$^+$) and EdU/Ki67-double-positive nuclei (EdU$^+$/Ki67$^+$) in the EGL region were quantified and graphed (n=3). Error bars represent mean±s.e.m. The P-value of each pair was calculated by t-test: A, $P\approx0.07$ (left graph), $P\approx0.02$ (right graph); B, $P\approx0.004$ (left graph), $P\leq0.0001$ (right graph). The number of EdU$^+$ nuclei reflects the proliferation state of EGL cells at the time point of EdU treatment. The Edu$^+$/Ki67$^+$ ratio reflects the proliferation state of EGL cells after one day of development. Dotted lines indicate the pial surface and areas marked in Fig. 6. Arrows indicate representitives of EdU-positive but Ki67-negative nuclei (Edu$^+$/Ki67$^-$). Scale bar=50 µm.

immunohistochemistry were taken under the Leica DMR or DM6000 microscope, respectively.

Histology, immunohistochemistry and TUNEL assay

Sagittal sections were prepared on either a Microtome (Microm HM325) or Cryostat (Leica CM1860C) at 10-12 µm each. Sections on the approximately same axial level were subjected to H&E staining or immunofluorescence staining with antibodies described in Table S7. Adjacent sections were subjected to terminal deoxynucleotidyl transferase dUTP nick end-labeling (TUNEL) assay using a detection system (Roche-Applied Science) according to the manufacturer's instructions.

EdU injection and labeling

Pregnant mice (E13.5, E14.5) were weighed and administrated with EdU (30 mg/kg) by intraperitoneal injection. Embryos were harvested 24 h after injections. Embryonic brains were dissected and fixed (4% PFA), then cryo-embedded in OCT. The embryonic brains were sectioned at 10 µm each. Sections were subjected to anti-Ki67 antibody staining, then EdU staining by using Click-iT Edu imaging kit (Life Technologies Inc.). Nuclei were counted and imaged under the Leica DMR and Carl-Zeiss LSM710.

FACS and immunofluorescence staining of primary cerebellar cells

E13.5 YFP$^+$ cerebellar primordia were dissociated by a modified protocol based on Wagner et al. (2011) and sorted by gating on the GFP channel of a BD FACSAria IIIu machine. The sorted YFP$^+$ cells were plated in a 24-well coated BD culture plate at a density of ~10,000 cells/well. The plated cells were slightly fixed by 4% PFA for 5 min and immunostained with antibodies against Pax2 and Rorα, and counter-stained with DAPI. Pax2$^+$ and Rorα$^+$ cells in ~30-40 microscopic fields (~1000 total cells) were counted and the ratios of Pax2$^+$/DAPI$^+$ and Rorα$^+$/DAPI$^+$ were determined for each sample.

RNA extraction, RT-qPCR and RNA-seq

Embryonic cerebellar primordia were precisely dissected and immediately immersed in 1 ml of RNAlater (Ambion/Life Technologies Inc.). Total RNA was extracted by using RNeasy Mini kit (Life Technologies Inc.) that yielded about 4-8 µg/sample. RNA aliquots of 500 ng were employed for reverse transcription (High-Capacity cDNA Reverse Transcription kit, Life Technologies Inc.) and reverse transcription quantitative PCR (RT-qPCR; SYBR Green PCR Master Mix, Life Technologies Inc.). RNA-seq libraries were generated with 2-4 µg RNA/sample using the TruSeq Kit (Illumina Inc.). The libraries were subsequently amplified by PCR and run in HiSeq™2000 (Illumina Inc.). RNA-seq was repeated with cerebella of four littermate controls and four Ezh2^{cKO} embryos (n=4, 4). Primers for RT-qPCR on *cdkn2a* transcipts were described in Juan et al. (2011).

ChIP-seq and ChIP-qPCR

Freshly dissected cerebellar primordia were cross-linked by 1% formaldehyde at room temperature for 15 min, washed twice with 0.1 M glycine-HCl, and immediately used for sonication or stored at −80°C. The cross-linked tissue was immersed in ChIP RIPA buffer (1× PBS, 1% NP40, 0.5% sodium deoxycholate, 0.1% SDS, Roche Protease Inhibitor Cocktail) in a 1.5 ml microcentrifuge tube on ice and sonicated by a Vibro-Cell Sonicator at 75% for 10×45 sec with 30 sec intervals for each cycle. Each cerebellar primordium yielded around 400-500 µg chromatin. ChIP-qPCR was performed with 40-50 µg chromatin and the remaining chromatin was processed for ChIP-seq with anti-H3K27me3 antibody. H3K27me3 ChIP-seq was repeated with cerebella of two littermate controls and Ezh2^{cKO} mice. The protocol for H3K27me3 ChIP-qPCR on the *Cdkn2a* promoter is described in Juan et al. (2011) and for ChIP-seq in Mousavi et al. (2012).

Bioinformatic analysis

For RNA-seq, raw sequences of 50 bp single-end reads were mapped to mouse genome (mm9 assembly) using TopHat (Trapnell et al., 2009) and gene transcript levels were determined via Cuffdiff in the form of FPKM (RPKM) values by correcting for multi reads and using geometric normalization (Trapnell et al., 2013). ChIP-seq data were mapped to the mouse genome (mm9 assembly) using the Bowtie algorithm (Langmead et al., 2009). Sequencing data generated from genomic DNA (input DNA) were used against the ChIP sample in calling enriched regions and to control for false discovery rate (FDR). Enriched regions for H3K27me3 were detected using the SICER algorithm at the FDR level of 5% with a window and gap size set to 200 bp and 600 bp, respectively (Zang et al., 2009). Downstream analyses to generate intensity profile around the transcriptional start site (TSS), and HeatMap for differentialy expressed genes and transcription factors were completed using custom written codes in

Development (2016) 143, 1971-1980 doi:10.1242/dev.132902

MATLAB and R, respectively. Gene ontology analyses were done using the online bioinformatics resource DAVID (National Institute of Allergy and Infectious Diseases, NIH) (Huang et al., 2009a,b).

MRI and Nissl stain

Adult mouse brains were imaged by the In Vivo NMR center at NIH MRI core facility on a 14 Tesla (Bruker Biospin Inc.) scanner. Images of frontal and dorsal optical sections were taken. Adult mouse brains were processed for Nissl staining according to Petralia and Wenthold (1999).

Acknowledgements

We thank Mario Capecchi and Alexander Tarakhovsky for sharing the *Pax7-Cre* and *Ezh2*$^{fl/fl}$ animals, respectively. Jim Simone and Jeffrey Lay helped with cell sorting, and Gustavo Gutierrez-Cruz assisted with sequencing. Members of the NIAMS Laboratory Animal Care and Use Section and NIAMS Light Imaging Section are kindly acknowledged. We thank Ya-xian Wang, Ron Petralia (NIDCD), Joe Laakso and John Hammer (NHLBI), Assia Derfoul and Stefania Dell'Orso (NIAMS) for technical help and advice. The Pax7 hybridoma (Kawakami et al., 1997) were obtained from the Developmental Studies Hybridoma Bank developed under the auspices of the NICHD and maintained by the Department of Biological Sciences, The University of Iowa, Iowa City, IA 52242, USA.

Competing interests

The authors declare no competing or financial interests.

Author contributions

X.F., A.H.J. and V.S. conceived the project. K.D.K. and H.Z. conducted computational analysis. X.F., A.H.J. and H.A.W. performed experiments. X.F. and V.S. wrote the manuscript.

Funding

This work was supported by the Intramural Research Program of the National Institute of Arthritis and Musculoskeletal and Skin Diseases (NIAMS) at the National Institutes of Health. Deposited in PMC for release after 12 months.

Data availability

The ChIP-seq and RNA-seq files related to the manuscript have been submitted and approved in GEO (http://www.ncbi.nlm.nih.gov/gds) with accession number GSE80222.

Supplementary information

Supplementary information available online at
http://dev.biologists.org/lookup/suppl/doi:10.1242/dev.132902/-/DC1

References

Bilovocky, N. A., Romito-DiGiacomo, R. R., Murcia, C. L., Maricich, S. M. and Herrup, K. (2003). Factors in the genetic background suppress the engrailed-1 cerebellar phenotype. *J. Neurosci.* **23**, 5105-5112.

Bouchard, M., Pfeffer, P. and Busslinger, M. (2000). Functional equivalence of the transcription factors Pax2 and Pax5 in mouse development. *Development* **127**, 3703-3713.

Boyer, L. A., Plath, K., Zeitlinger, J., Brambrink, T., Medeiros, L. A., Lee, T. I., Levine, S. S., Wernig, M., Tajonar, A., Ray, M. K. et al. (2006). Polycomb complexes repress developmental regulators in murine embryonic stem cells. *Nature* **441**, 349-353.

Bracken, A. P., Kleine-Kohlbrecher, D., Dietrich, N., Pasini, D., Gargiulo, G., Beekman, C., Theilgaard-Monch, K., Minucci, S., Porse, B. T., Marine, J.-C. et al. (2007). The Polycomb group proteins bind throughout the INK4A-ARF locus and are disassociated in senescent cells. *Genes Dev.* **21**, 525-530.

Cao, R., Wang, L., Wang, H., Xia, L., Erdjument-Bromage, H., Tempst, P., Jones, R. S. and Zhang, Y. (2002). Role of histone H3 lysine 27 methylation in Polycomb-group silencing. *Science* **298**, 1039-1043.

Cheng, Y., Sudarov, A., Szulc, K. U., Sgaier, S. K., Stephen, D., Turnbull, D. H. and Joyner, A. L. (2010). The Engrailed homeobox genes determine the different foliation patterns in the vermis and hemispheres of the mammalian cerebellum. *Development* **137**, 519-529.

Chi, C. L., Martinez, S., Wurst, W. and Martin, G. R. (2003). The isthmic organizer signal FGF8 is required for cell survival in the prospective midbrain and cerebellum. *Development* **130**, 2633-2644.

Corrales, J. D., Rocco, G. L., Blaess, S., Guo, Q. and Joyner, A. L. (2004). Spatial pattern of sonic hedgehog signaling through Gli genes during cerebellum development. *Development* **131**, 5581-5590.

Crossley, P. H., Minowada, G., MacArthur, C. A. and Martin, G. R. (1996). Roles for FGF8 in the induction, initiation, and maintenance of chick limb development. *Cell* **84**, 127-136.

Dalgard, C. L., Zhou, Q., Lundell, T. G. and Doughty, M. L. (2011). Altered gene expression in the emerging cerebellar primordium of Neurog1-/- mice. *Brain Res.* **1388**, 12-21.

Di Meglio, T., Kratochwil, C. F., Vilain, N., Loche, A., Vitobello, A., Yonehara, K., Hrycaj, S. M., Roska, B., Peters, A. H. F. M., Eichmann, A. et al. (2013). Ezh2 orchestrates topographic migration and connectivity of mouse precerebellar neurons. *Science* **339**, 204-207.

Engelkamp, D., Rashbass, P., Seawright, A. and van Heyningen, V. (1999). Role of Pax6 in development of the cerebellar system. *Development* **126**, 3585-3596.

Englund, C., Kowalczyk, T., Daza, R. A. M., Dagan, A., Lau, C., Rose, M. F. and Hevner, R. F. (2006). Unipolar brush cells of the cerebellum are produced in the rhombic lip and migrate through developing white matter. *J. Neurosci.* **26**, 9184-9195.

Ezhkova, E., Pasolli, H. A., Parker, J. S., Stokes, N., Su, I.-H., Hannon, G., Tarakhovsky, A. and Fuchs, E. (2009). Ezh2 orchestrates gene expression for the stepwise differentiation of tissue-specific stem cells. *Cell* **136**, 1122-1135.

Fujita, H. and Sugihara, I. (2012). FoxP2 expression in the cerebellum and inferior olive: development of the transverse stripe-shaped expression pattern in the mouse cerebellar cortex. *J. Comp. Neurol.* **520**, 656-677.

Gold, D. A., Baek, S. H., Schork, N. J., Rose, D. W., Larsen, D. D., Sachs, B. D., Rosenfeld, M. G. and Hamilton, B. A. (2003). RORalpha coordinates reciprocal signaling in cerebellar development through sonic hedgehog and calcium-dependent pathways. *Neuron* **40**, 1119-1131.

Hamilton, B. A., Frankel, W. N., Kerrebrock, A. W., Hawkins, T. L., FitzHugh, W., Kusumi, K., Russell, L. B., Mueller, K. L., van Berkel, V., Birren, B. W. et al. (1996). Disruption of the nuclear hormone receptor RORalpha in staggerer mice. *Nature* **379**, 736-739.

He, A., Ma, Q., Cao, J., von Gise, A., Zhou, P., Xie, H., Zhang, B., Hsing, M., Christodoulou, D. C., Cahan, P. et al. (2012). Polycomb repressive complex 2 regulates normal development of the mouse heart. *Circ. Res.* **110**, 406-415.

Hirabayashi, Y., Suzki, N., Tsuboi, M., Endo, T. A., Toyoda, T., Shinga, J., Koseki, H., Vidal, M. and Gotoh, Y. (2009). Polycomb limits the neurogenic competence of neural precursor cells to promote astrogenic fate transition. *Neuron* **63**, 600-613.

Hoshino, M., Nakamura, S., Mori, K., Kawauchi, T., Terao, M., Nishimura, Y. V., Fukuda, A., Fuse, T., Matsuo, N., Sone, M. et al. (2005). Ptf1a, a bHLH transcriptional gene, defines GABAergic neuronal fates in cerebellum. *Neuron* **47**, 201-213.

Huang, D. W., Sherman, B. T. and Lempicki, R. A. (2009a). Bioinformatics enrichment tools: paths toward the comprehensive functional analysis of large gene lists. *Nucleic Acids Res.* **37**, 1-13.

Huang, D. W., Sherman, B. T. and Lempicki, R. A. (2009b). Systematic and integrative analysis of large gene lists using DAVID Bioinformatics Resources. *Nat. Protoc.* **4**, 44-57.

Jostes, B., Walther, C. and Gruss, P. (1990). The murine paired box gene, Pax7, is expressed specifically during the development of the nervous and muscular system. *Mech. Dev.* **33**, 27-37.

Joyner, A. L., Herrup, K., Auerbach, B. A., Davis, C. A. and Rossant, J. (1991). Subtle cerebellar phenotype in mice homozygous for a targeted deletion of the En-2 homeobox. *Science* **251**, 1239-1243.

Juan, A. H., Derfoul, A., Feng, X., Ryall, J. G., Dell'Orso, S., Pasut, A., Zare, H., Simone, J. M., Rudnicki, M. A. and Sartorelli, V. (2011). Polycomb EZH2 controls self-renewal and safeguards the transcriptional identity of skeletal muscle stem cells. *Genes Dev.* **25**, 789-794.

Kawakami, A., Kimura-Kawakami, M., Nomura, T. and Fujisawa, H. (1997). Distributions of PAX6 and PAX7 proteins suggest their involvement in both early and late phases of chick brain development. *Mech. Dev.* **66**, 119-130.

Keller, C., Hansen, M. S., Coffin, C. M. and Capecchi, M. R. (2004). Pax3:Fkhr interferes with embryonic Pax3 and Pax7 function: implications for alveolar rhabdomyosarcoma cell of origin. *Genes Dev.* **18**, 2608-2613.

Kim, E. J., Hori, K., Wyckoff, A., Dickel, L. K., Koundakjian, E. J., Goodrich, L. V. and Johnson, J. E. (2011). Spatiotemporal fate map of neurogenin1 (Neurog1) lineages in the mouse central nervous system. *J. Comp. Neurol.* **519**, 1355-1370.

Kirmizis, A., Bartley, S. M., Kuzmichev, A., Margueron, R., Reinberg, D., Green, R. and Farnham, P. J. (2004). Silencing of human polycomb target genes is associated with methylation of histone H3 Lys 27. *Genes Dev.* **18**, 1592-1605.

Kuzmichev, A., Nishioka, K., Erdjument-Bromage, H., Tempst, P. and Reinberg, D. (2002). Histone methyltransferase activity associated with a human multiprotein complex containing the Enhancer of Zeste protein. *Genes Dev.* **16**, 2893-2905.

Langmead, B., Trapnell, C., Pop, M. and Salzberg, S. L. (2009). Ultrafast and memory-efficient alignment of short DNA sequences to the human genome. *Genome Biol.* **10**, R25.

Laugesen, A. and Helin, K. (2014). Chromatin repressive complexes in stem cells, development, and cancer. *Cell Stem Cell* **14**, 735-751.

Leung, C., Lingbeek, M., Shakhova, O., Liu, J., Tanger, E., Saremaslani, P., Van Lohuizen, M. and Marino, S. (2004). Bmi1 is essential for cerebellar development and is overexpressed in human medulloblastomas. *Nature* **428**, 337-341.

Lewis, P. M., Gritli-Linde, A., Smeyne, R., Kottmann, A. and McMahon, A. P. (2004). Sonic hedgehog signaling is required for expansion of granule neuron precursors and patterning of the mouse cerebellum. *Dev. Biol.* **270**, 393-410.
Li, J. Y. and Joyner, A. L. (2001). Otx2 and Gbx2 are required for refinement and not induction of mid-hindbrain gene expression. *Development* **128**, 4979-4991.
Li, J., Hart, R. P., Mallimo, E. M., Swerdel, M. R., Kusnecov, A. W. and Herrup, K. (2013). EZH2-mediated H3K27 trimethylation mediates neurodegeneration in ataxia-telangiectasia. *Nat. Neurosci.* **16**, 1745-1753.
Liu, A. and Joyner, A. L. (2001). EN and GBX2 play essential roles downstream of FGF8 in patterning the mouse mid/hindbrain region. *Development* **128**, 181-191.
Machold, R. and Fishell, G. (2005). Math1 is expressed in temporally discrete pools of cerebellar rhombic-lip neural progenitors. *Neuron* **48**, 17-24.
Maricich, S. M. and Herrup, K. (1999). Pax-2 expression defines a subset of GABAergic interneurons and their precursors in the developing murine cerebellum. *J. neurobiol.* **41**, 281-294.
Martinez, S., Crossley, P. H., Cobos, I., Rubenstein, J. L. and Martin, G. R. (1999). FGF8 induces formation of an ectopic isthmic organizer and isthmocerebellar development via a repressive effect on Otx2 expression. *Development* **126**, 1189-1200.
Martinez, S., Andreu, A., Mecklenburg, N. and Echevarria, D. (2013). Cellular and molecular basis of cerebellar development. *Front. Neuroanat.* **7**, 18.
Marzban, H., Del Bigio, M. R., Alizadeh, J., Ghavami, S., Zachariah, R. M. and Rastegar, M. (2014). Cellular commitment in the developing cerebellum. *Front Cell Neurosci.* **8**, 450.
Meyers, E. N., Lewandoski, M. and Martin, G. R. (1998). An Fgf8 mutant allelic series generated by Cre- and Flp-mediated recombination. *Nat. Genet.* **18**, 136-141.
Millen, K. J., Wurst, W., Herrup, K. and Joyner, A. L. (1994). Abnormal embryonic cerebellar development and patterning of postnatal foliation in two mouse Engrailed-2 mutants. *Development* **120**, 695-706.
Millen, K. J., Hui, C. C. and Joyner, and A. L. (1995). A role for En-2 and other murine homologues of Drosophila segment polarity genes in regulating positional information in the developing cerebellum. *Development* **121**, 3935-3945.
Millen, K. J., Steshina, E. Y., Iskusnykh, I. Y. and Chizhikov, V. V. (2014). Transformation of the cerebellum into more ventral brainstem fates causes cerebellar agenesis in the absence of Ptf1a function. *Proc. Natl. Acad. Sci. USA* **111**, E1777-E1786.
Minaki, Y., Nakatani, T., Mizuhara, E., Inoue, T. and Ono, Y. (2008). Identification of a novel transcriptional corepressor, Corl2, as a cerebellar Purkinje cell-selective marker. *Gene Expr. Patterns* **8**, 418-423.
Mousavi, K., Zare, H., Wang, A. H. and Sartorelli, V. (2012). Polycomb protein Ezh1 promotes RNA polymerase II elongation. *Mol. Cell* **45**, 255-262.
Nakagawa, S., Watanabe, M. and Inoue, Y. (1997). Prominent expression of nuclear hormone receptor ROR alpha in Purkinje cells from early development. *Neurosci. Res.* **28**, 177-184.
Nakatani, T., Minaki, Y., Kumai, M., Nitta, C. and Ono, Y. (2014). The c-Ski family member and transcriptional regulator Corl2/Skor2 promotes early differentiation of cerebellar Purkinje cells. *Dev. Biol.* **388**, 68-80.
Nobori, T., Miura, K., Wu, D. J., Lois, A., Takabayashi, K. and Carson, D. A. (1994). Deletions of the cyclin-dependent kinase-4 inhibitor gene in multiple human cancers. *Nature* **368**, 753-756.
O'Carroll, D., Erhardt, S., Pagani, M., Barton, S. C., Surani, M. A. and Jenuwein, T. (2001). The polycomb-group gene Ezh2 is required for early mouse development. *Mol. Cell. Biol.* **21**, 4330-4336.
Parisi, M. A. and Dobyns, W. B. (2003). Human malformations of the midbrain and hindbrain: review and proposed classification scheme. *Mol. Genet. Metab.* **80**, 36-53.
Pascual, M., Abasolo, I., Mingorance-Le Meur, A., Martinez, A., Del Rio, J. A., Wright, C. V. E., Real, F. X. and Soriano, E. (2007). Cerebellar GABAergic progenitors adopt an external granule cell-like phenotype in the absence of Ptf1a transcription factor expression. *Proc. Natl. Acad. Sci. USA* **104**, 5193-5198.
Pereira, J. D., Sansom, S. N., Smith, J., Dobenecker, M.-W., Tarakhovsky, A. and Livesey, F. J. (2010). Ezh2, the histone methyltransferase of PRC2, regulates the balance between self-renewal and differentiation in the cerebral cortex. *Proc. Natl. Acad. Sci. USA* **107**, 15957-15962.
Petralia, R. S. and Wenthold, R. J. (1999). Immunocytochemistry of NMDA receptors. *Methods Mol. Biol.* **128**, 73-92.
Pillai, A., Mansouri, A., Behringer, R., Westphal, H. and Goulding, M. (2007). Lhx1 and Lhx5 maintain the inhibitory-neurotransmitter status of interneurons in the dorsal spinal cord. *Development* **134**, 357-366.
Roussel, M. F. and Hatten, M. E. (2011). Cerebellum development and medulloblastoma. *Curr. Top. Dev. Biol.* **94**, 235-282.
Seale, P., Sabourin, L. A., Girgis-Gabardo, A., Mansouri, A., Gruss, P. and Rudnicki, M. A. (2000). Pax7 is required for the specification of myogenic satellite cells. *Cell* **102**, 777-786.
Sellick, G. S., Barker, K. T., Stolte-Dijkstra, I., Fleischmann, C., Coleman, R. J., Garrett, C., Gloyn, A. L., Edghill, E. L., Hattersley, A. T., Wellauer, P. K. et al. (2004). Mutations in PTF1A cause pancreatic and cerebellar agenesis. *Nat. Genet.* **36**, 1301-1305.
Seto, Y., Nakatani, T., Masuyama, N., Taya, S., Kumai, M., Minaki, Y., Hamaguchi, A., Inoue, Y. U., Inoue, T., Miyashita, S. et al. (2014). Temporal identity transition from Purkinje cell progenitors to GABAergic interneuron progenitors in the cerebellum. *Nat. Commun.* **5**, 3337.
Snitow, M. E., Li, S., Morley, M. P., Rathi, K., Lu, M. M., Kadzik, R. S., Stewart, K. M. and Morrisey, E. E. (2015). Ezh2 represses the basal cell lineage during lung endoderm development. *Development* **142**, 108-117.
Srinivas, S., Watanabe, T., Lin, C.-S., William, C. M., Tanabe, Y., Jessell, T. M. and Costantini, F. (2001). Cre reporter strains produced by targeted insertion of EYFP and ECFP into the ROSA26 locus. *BMC Dev. Biol.* **1**, 4.
Su, I.-H., Basavaraj, A., Krutchinsky, A. N., Hobert, O., Ullrich, A., Chait, B. T. and Tarakhovsky, A. (2003). Ezh2 controls B cell development through histone H3 methylation and Igh rearrangement. *Nat. Immunol.* **4**, 124-131.
Sudarov, A., Turnbull, R. K., Kim, E. J., Lebel-Potter, M., Guillemot, F. and Joyner, A. L. (2011). Ascl1 genetics reveals insights into cerebellum local circuit assembly. *J. Neurosci.* **31**, 11055-11069.
Trapnell, C., Pachter, L. and Salzberg, S. L. (2009). TopHat: discovering splice junctions with RNA-Seq. *Bioinformatics* **25**, 1105-1111.
Trapnell, C., Hendrickson, D. G., Sauvageau, M., Goff, L., Rinn, J. L. and Pachter, L. (2013). Differential analysis of gene regulation at transcript resolution with RNA-seq. *Nat. Biotechnol.* **31**, 46-53.
Wagner, W., McCroskery, S. and Hammer, J. A. 3rd (2011). An efficient method for the long-term and specific expression of exogenous cDNAs in cultured Purkinje neurons. *J. Neurosci. Methods* **200**, 95-105.
Wang, V. Y., Rose, M. F. and Zoghbi, H. Y. (2005). Math1 expression redefines the rhombic lip derivatives and reveals novel lineages within the brainstem and cerebellum. *Neuron* **48**, 31-43.
Wei, P., Blundon, J. A., Rong, Y., Zakharenko, S. S. and Morgan, J. I. (2011). Impaired locomotor learning and altered cerebellar synaptic plasticity in pep-19/PCP4-null mice. *Mol. Cell. Biol.* **31**, 2838-2844.
Weisheit, G., Gliem, M., Endl, E., Pfeffer, P. L., Busslinger, M. and Schilling, K. (2006). Postnatal development of the murine cerebellar cortex: formation and early dispersal of basket, stellate and Golgi neurons. *Eur. J. Neurosci.* **24**, 466-478.
Woodhouse, S., Pugazhendhi, D., Brien, P. and Pell, J. M. (2013). Ezh2 maintains a key phase of muscle satellite cell expansion but does not regulate terminal differentiation. *J. Cell Sci.* **126**, 565-579.
Wurst, W., Auerbach, A. B. and Joyner, A. L. (1994). Multiple developmental defects in Engrailed-1 mutant mice: an early mid-hindbrain deletion and patterning defects in forelimbs and sternum. *Development* **120**, 2065-2075.
Young, R. A. (2011). Control of the embryonic stem cell state. *Cell* **144**, 940-954.
Zang, C., Schones, D. E., Zeng, C., Cui, K., Zhao, K. and Peng, W. (2009). A clustering approach for identification of enriched domains from histone modification ChIP-Seq data. *Bioinformatics* **25**, 1952-1958.
Zeng, C., Pan, F., Jones, L. A., Lim, M. M., Griffin, E. A., Sheline, Y. I., Mintun, M. A., Holtzman, D. M. and Mach, R. H. (2010). Evaluation of 5-ethynyl-2′-deoxyuridine staining as a sensitive and reliable method for studying cell proliferation in the adult nervous system. *Brain Res.* **1319**, 21-32.
Zervas, M., Blaess, S. and Joyner, A. L. (2005). Classical embryological studies and modern genetic analysis of midbrain and cerebellum development. *Curr. Top. Dev. Biol.* **69**, 101-138.
Zhao, Y., Kwan, K.-M., Mailloux, C. M., Lee, W.-K., Grinberg, A., Wurst, W., Behringer, R. R. and Westphal, H. (2007). LIM-homeodomain proteins Lhx1 and Lhx5, and their cofactor Ldb1, control Purkinje cell differentiation in the developing cerebellum. *Proc. Natl. Acad. Sci. USA* **104**, 13182-13186.

Supplemental Material

Table S1: The list of genes whose promoter regions were occupied by H3K27me3 in E13.5 cerebella.

Click here to Download Table S1

Table S2: The list of genes that were up- and down-regulated in E13.5 Ezh2^{cKO} cerebella.

Click here to Download Table S2

Table S3: The list of genes that were up-regulated in E13.5 Ezh2^{cKO} cerebella and their promoter regions were also occupied by H3K27me3.

Click here to Download Table S3

Table S4: The GO analysis of up-regulated genes in E13.5 Ezh2^{cKO} cerebella

Click here to Download Table S4

Table S5: The GO analysis of down-regulated genes in E13.5 Ezh2^{cKO} cerebella

Click here to Download Table S5

Table S6: The list of Purkinje-specific "membrane" genes that were down-regulated in Ezh2^{cKO} cerebella

Gene Name	Reference
Plxdc2/TEM7R	(1)
Car8	(2)
CAPS2/CADPS2	(3)
KCNA4	(4)
KCNIP4	(5)
KCNJ3/GIRK1	(6)
Slitrk6	(7)
EBF2	(8, 9)
SPHK1	(10)
SCA12/PP2R2B	(11)
PSD-93/Chapsyn-110	(12)
11 X-linked	(13)
SLC1A6/EAAT4	(14)
Pla2g4e	(15)
neuropilin-2	(16)
HAS2	(17)

1. Miller SF, *et al.* (2007) Expression of Plxdc2/TEM7R in the developing nervous system of the mouse. *Gene expression patterns : GEP* 7(5):635-644.
2. Lakkis MM, O'Shea KS, & Tashian RE (1997) Differential expression of the carbonic anhydrase genes for CA VII (Car7) and CA-RP VIII (Car8) in mouse brain. *The journal of histochemistry and cytochemistry : official journal of the Histochemistry Society* 45(5):657-662.
3. Sadakata T, *et al.* (2007) Impaired cerebellar development and function in mice lacking CAPS2, a protein involved in neurotrophin release. *The Journal of neuroscience : the official journal of the Society for Neuroscience* 27(10):2472-2482.
4. Chung YH, Shin C, Kim MJ, Lee BK, & Cha CI (2001) Immunohistochemical study on the distribution of six members of the Kv1 channel subunits in the rat cerebellum. *Brain research* 895(1-2):173-177.
5. Xiong H, Kovacs I, & Zhang Z (2004) Differential distribution of KChIPs mRNAs in adult mouse brain. *Brain research. Molecular brain research* 128(2):103-111.
6. Fernandez-Alacid L, *et al.* (2009) Subcellular compartment-specific molecular diversity of pre- and post-synaptic GABA-activated GIRK channels in Purkinje cells. *Journal of neurochemistry* 110(4):1363-1376.
7. Aruga J (2003) Slitrk6 expression profile in the mouse embryo and its relationship to that of Nlrr3. *Gene expression patterns : GEP* 3(6):727-733.

8. Croci L, *et al.* (2011) Local insulin-like growth factor I expression is essential for Purkinje neuron survival at birth. *Cell death and differentiation* 18(1):48-59.
9. Chung SH, Marzban H, Croci L, Consalez GG, & Hawkes R (2008) Purkinje cell subtype specification in the cerebellar cortex: early B-cell factor 2 acts to repress the zebrin II-positive Purkinje cell phenotype. *Neuroscience* 153(3):721-732.
10. Terada N, *et al.* (2004) Compartmentation of the mouse cerebellar cortex by sphingosine kinase. *The Journal of comparative neurology* 469(1):119-127.
11. Strack S, Zaucha JA, Ebner FF, Colbran RJ, & Wadzinski BE (1998) Brain protein phosphatase 2A: developmental regulation and distinct cellular and subcellular localization by B subunits. *The Journal of comparative neurology* 392(4):515-527.
12. Brenman JE, *et al.* (1998) Localization of postsynaptic density-93 to dendritic microtubules and interaction with microtubule-associated protein 1A. *The Journal of neuroscience : the official journal of the Society for Neuroscience* 18(21):8805-8813.
13. Priddle TH & Crow TJ (2013) Protocadherin 11X/Y a human-specific gene pair: an immunohistochemical survey of fetal and adult brains. *Cerebral cortex* 23(8):1933-1941.
14. Dehnes Y, *et al.* (1998) The glutamate transporter EAAT4 in rat cerebellar Purkinje cells: a glutamate-gated chloride channel concentrated near the synapse in parts of the dendritic membrane facing astroglia. *The Journal of neuroscience : the official journal of the Society for Neuroscience* 18(10):3606-3619.
15. Shirai Y & Ito M (2004) Specific differential expression of phospholipase A2 subtypes in rat cerebellum. *Journal of neurocytology* 33(3):297-307.
16. Chen H, Chedotal A, He Z, Goodman CS, & Tessier-Lavigne M (1997) Neuropilin-2, a novel member of the neuropilin family, is a high affinity receptor for the semaphorins Sema E and Sema IV but not Sema III. *Neuron* 19(3):547-559.
17. Carulli D, Rhodes KE, & Fawcett JW (2007) Upregulation of aggrecan, link protein 1, and hyaluronan synthases during formation of perineuronal nets in the rat cerebellum. *The Journal of comparative neurology* 501(1):83-94.

Table S7: The list of antibodies used in this study

Primary Antibodies	Company	Cat. #	Dilution	Antigen retrival
Pax7 (mouse monoclonal)	Developmental Studies Hybridoma Bank		1: 5	Yes
H3K27me3 (rabbit polyclonal)	Millipore Inc.	07-449	1: 400	No
Ezh2 (rabbit polyclonal)	Active Motif Inc.	39901	1: 400	Yes
Ki67 (rabbit polyclonal)	Abcam Inc.	ab15580	1: 400	Yes
Pax2 (rabbit polyclonal)	Invitrogen Inc.	71-6000	1: 400	Yes
RoRa (rabbit polyclonal)	Santa Cruz Biotechnology Inc.	sc-28612	1: 50	Yes
Pax6 (rabbit polyclonal)	BioLegend Inc.	PRB-278P	1: 400	Yes
Cdkn2a a.k.a. p16 (F-4)	Stanta Cruz Biotechnology Inc.	Sc-74401	1: 50	No

Secondary Antibodies	Company	Cat.#	Dilution
Goat Anti-Mouse IgG1(Alexa Fluor® 488)	Life Technologies Inc.	A-21121	1: 800
Goat Anti-Rabbit IgG H&L (Alexa Fluor® 488)	Life Technologies Inc.	A-11034	1: 800
Goat Anti-Rabbit IgG H&L (Alexa Fluor® 555)	Life Technologies Inc.	A-21428	1: 800

Figures:

Supplemental Figure S1. (A) Nissl stain of adult control and Ezh2^{cKO} cerebella sectioned by vibrotome. (B) MRI images of adult mouse brain. Upper panels are frontal views. Lower panels are top views. The arrows point to the position of vermis (V).

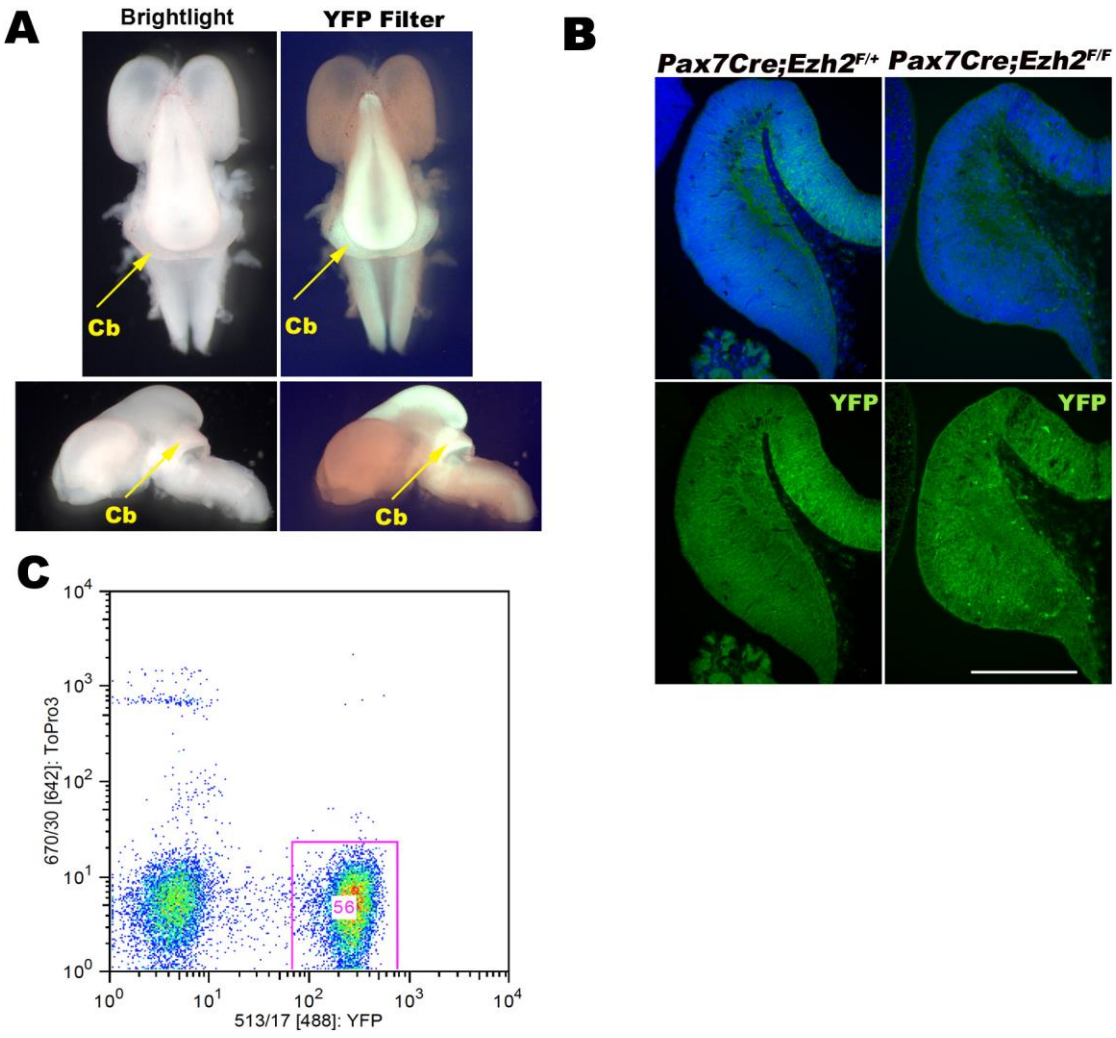

Supplemental Figure S2. (A) The left panel is the image of the E13.5 brain dissected from Ezh2$^{cKO:YFP}$ embryo under bright field microscope. Right panel is an image of the same embryonic brain under a fluorescent microscope revealing YFP^{+} regions including the embryonic cerebellum (Cb). The upper panels are dorsal view; the lower panels are lateral view. (B) Sagittal sections of E13.5 YFP+ embryos in the study including both littermate control (left) and Ezh2$^{cKO:YFP}$ embryo (right) (C) FACS graph showing the sorted YFP^{+} cells from disassociated Ezh2$^{cKO:YFP}$ cerebella.

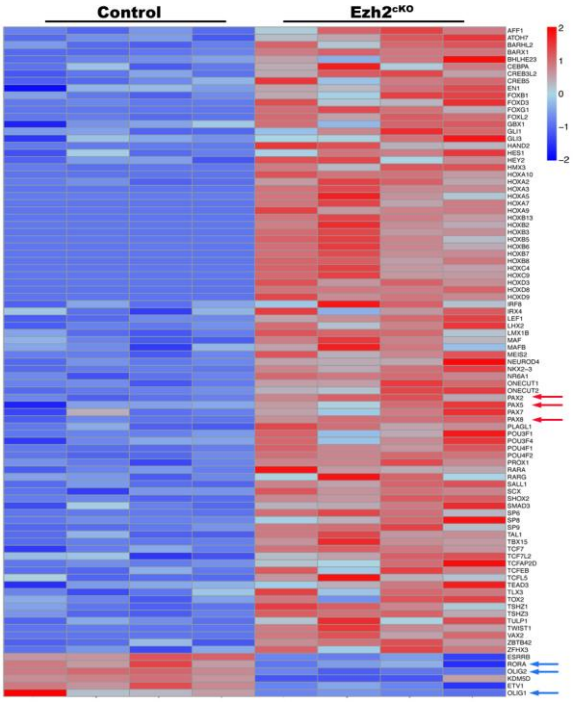

Supplemental Figure S3. Heat-map representing expression of transcription factors exhibiting changes between Ezh2^{cKO} and its littermate control. Arrows point to transcription factors involved in PC and IN commitment and differentiation.

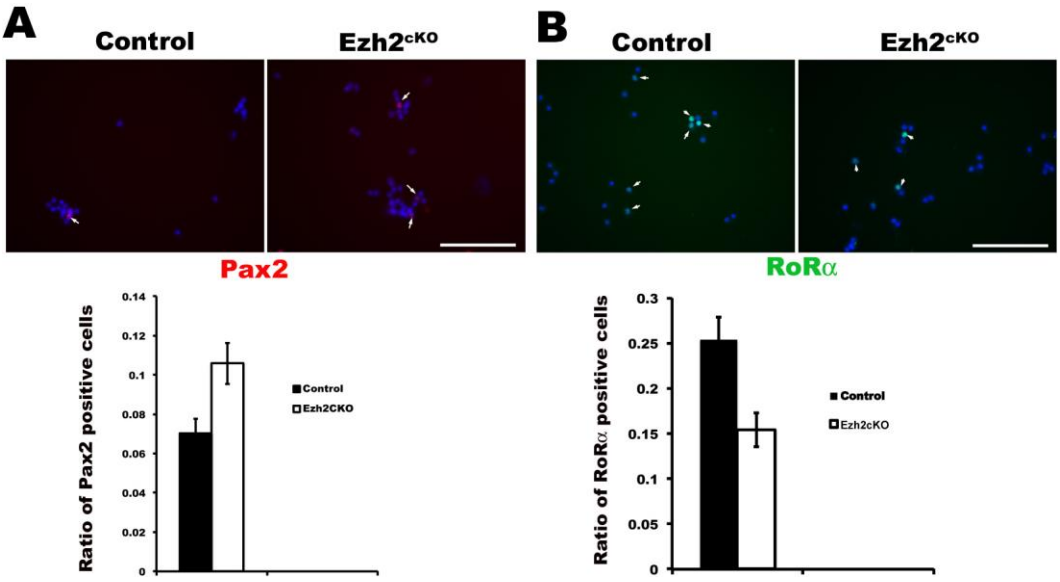

Supplemental Figure S4. (A) FACS-sorted E13.5 YFP^{+} cerebellar cells were immunostained with Pax2 antibody (red) and counterstained with DAPI (blue). The Pax2^{+} cells were counted and normalized by total DAPI^{+} cells (~1000/ sample, 2 controls and 3 Ezh2^{cKO}) and graphed. Bars represent mean ± SEM. (B) FACS-sorted E13.5 YFP^{+} cerebellar cells were immunostained with RoRα antibody (green) and counterstained with DAPI (blue). The RoRa^{+} cells were counted and normalized by total DAPI^{+} cells (~1000/ sample, 2 controls and 3 Ezh2^{cKO}) and graphed. Error bars represent mean ± SEM.

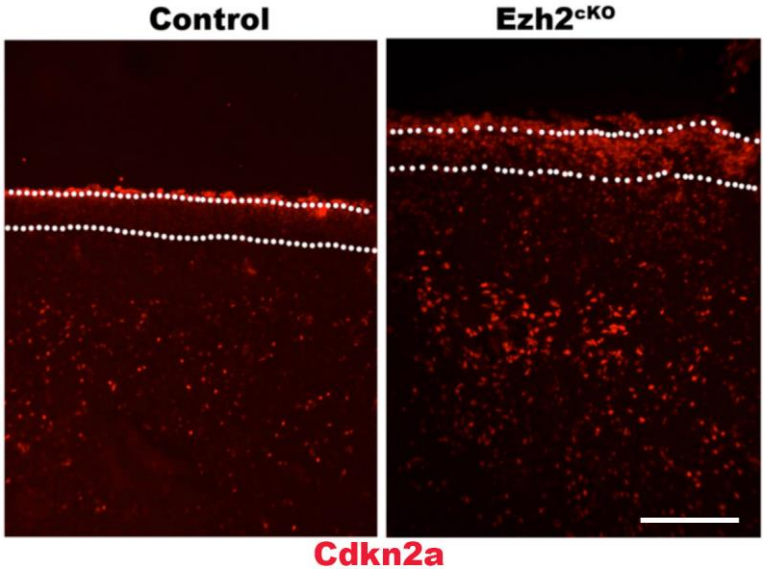

Supplemental Figure S5. Coronal sections of embryonic cerebellum (E17.5) were immunostained with Cdkn2a (p16) antibody. The dotted lines mark the EGL region of control and Ezh2^{cKO}.

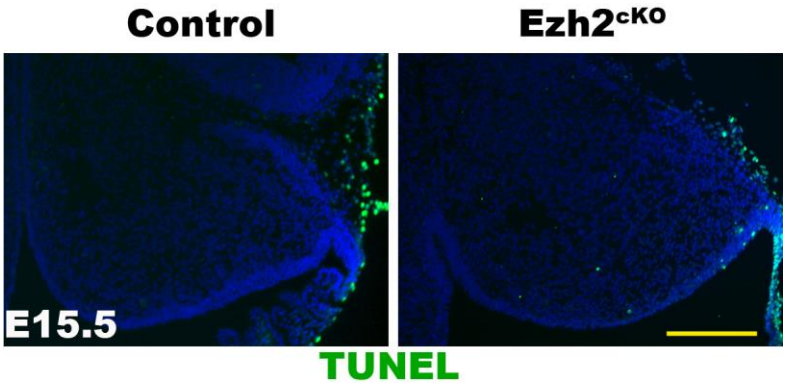

Supplemental Figure S6. TUNEL assay on sagittal sections of E15.5 cerebellar of Ezh2^{cKO} and its littermate control